

Mutation in a non-force-bearing region of protein L influences force-dependent unfolding behavior

Huanjie Jiang(蒋环杰), Yanwei Wang(王艳伟), Jiayuan Chen(陈家媛), Dan Hu(胡丹), Hai Pan(潘海), Zilong Guo(郭子龙), and Hu Chen(陈虎)

Citation: Chin. Phys. B, 2024, 33 (**7**): 078201. DOI: 10.1088/1674-1056/ad3dcd
Journal homepage: http://cpb.iphy.ac.cn; http://iopscience.iop.org/cpb

What follows is a list of articles you may be interested in

Concerted versus stepwise mechanisms of cyclic proton transfer: Experiments, simulations, and current challenges

Yi-Han Cheng(程奕涵), Yu-Cheng Zhu(朱禹丞), Xin-Zheng Li(李新征), and Wei Fang(方为)
Chin. Phys. B, 2023, 32 (**1**): 018201. DOI: 10.1088/1674-1056/ac98a5

Single-molecule mechanical folding and unfolding kinetics of armless mitochondrial $tRNA^{Arg}$ from *Romanomermis culicivorax*

Yan-Hui Li(李彦慧), Zhen-Sheng Zhong(钟振声), and Jie Ma(马杰)
Chin. Phys. B, 2021, 30 (**10**): 108203. DOI: 10.1088/1674-1056/ac1e1e

Equilibrium folding and unfolding dynamics to reveal detailed free energy landscape of src SH3 protein by magnetic tweezers

Huanhuan Su(苏环环), Hao Sun(孙皓), Haiyan Hong(洪海燕), Zilong Guo(郭子龙), Ping Yu(余平), and Hu Chen(陈虎)
Chin. Phys. B, 2021, 30 (**7**): 078201. DOI: 10.1088/1674-1056/abfb56

Theoretical investigation on the excited state intramolecular proton transfer in Me_2N substituted flavonoid by the time-dependent density functional theory method

Hang Yin(尹航), Ying Shi(石英)
Chin. Phys. B, 2018, 27 (**5**): 058201. DOI: 10.1088/1674-1056/27/5/058201

Direct observation of λ -DNA molecule reversal movement within microfluidic channels under electric field with single molecule imaging technique

Fengyun Yang(杨凤云), Kaige Wang(王凯歌), Dan Sun(孙聃), Wei Zhao(赵伟), Hai-qing Wang(王海青), Xin He(何鑫), Gui-ren Wang(王归仁), Jin-tao Bai(白晋涛)
Chin. Phys. B, 2016, 25 (**7**): 078201. DOI: 10.1088/1674-1056/25/7/078201

Mutation in a non-force-bearing region of protein L influences force-dependent unfolding behavior

Huanjie Jiang(蒋环杰)[1,2], Yanwei Wang(王艳伟)[1], Jiayuan Chen(陈家媛)[1,2], Dan Hu(胡丹)[1,2], Hai Pan(潘海)[2], Zilong Guo(郭子龙)[2], and Hu Chen(陈虎)[2,3,†]

[1] *Department of Physics, Wenzhou University, Wenzhou* 325035, *China*
[2] *Center of Biomedical Physics, Wenzhou Institute, University of Chinese Academy of Sciences, Wenzhou* 325000, *China*
[3] *Research Institute for Biomimetics and Soft Matter, Fujian Provincial Key Laboratory for Soft Functional Materials Research, Department of Physics, Xiamen University, Xiamen* 361005, *China*

(Received 25 January 2024; revised manuscript received 18 March 2024; accepted manuscript online 12 April 2024)

Single-molecule magnetic tweezers (MTs) have revealed multiple transition barriers along the unfolding pathway of several two-state proteins, such as GB1 and Csp. In this study, we utilized MTs to measure the force-dependent folding and unfolding rates of both protein L (PLWT) and its Y47W mutant (PLY47W) where the mutation point is not at the force-bearing β-strands. The measurements were conducted within a force range of 3–120 pN. Notably, the unfolding rates of both PLWT and PWY47W exhibit distinct force sensitivities below 50 pN and above 60 pN, implying a two-barrier free energy landscape. Both PLWT and PLY47W share the same force-dependent folding rate and the same transition barriers, but the unfolding rate of PLY47W is faster than that of PLWT. Our finding demonstrates that the residue outside of the force-bearing region will also affect the force-induced unfolding dynamics.

Keywords: protein folding, magnetic tweezers, protein L

PACS: 82.37.Rs, 82.20.Db, 87.15.R–, 87.14.E– **DOI:** 10.1088/1674-1056/ad3dcd

1. Introduction

The protein folding problem remains a challenge in molecular biology due to the vast conformation space of polypeptide chains and incomplete understanding of the underlying mechanisms governing protein folding and unfolding.[1,2]

Small globular proteins, such as protein L, GB1, Csp, and spectrin serve as essential models for investigating protein folding in chemical and mechanical denatured experiments.[3–8] The composition of secondary structures and the topological structure of these globular proteins affect their folding dynamics.[9] The wild type of protein L (PLWT) and its Y47W mutant (PLY47W) have globular structures with one α-helix and four β-strands, which have been resolved with protein data bank ID 2PTL and 1HZ6, respectively. PLY47W exhibits superior intrinsic fluorescence properties compared to PLWT. As a result, the folding and unfolding dynamics of PLY47W have been extensively investigated by chemical denaturation method. David Baker *et al.* used the stopped-flow technique to measure the folding and unfolding rates of PLY47W in guanidine hydrochloride (GuHCl) solutions,[4] and obtained a 'chevron plot' that quantitatively showed how the unfolding and refolding rates depend on the GuHCl concentration in solution. The measurements on PLY47W and other mutants of protein L revealed that one of the two β-turns of the protein was formed and the other was disrupted in the folding transition state.[10]

Recently, single-molecule force spectroscopy (SMFS) has emerged as a powerful tool for investigating conformation changes of proteins.[11,12] Force-dependent unfolding and folding rates of PLY47W have been measured by atomic force microscopy (AFM) and magnetic tweezers (MTs).[10,13] In these studies, Bell's model is employed to explain the unfolding force distribution obtained from constant pulling speed experiments, or to fit force-dependent unfolding rates from constant force experiments:[2,14]

$$k_{\mathrm{u}}(f) = k_{\mathrm{u}}^{0} \exp(f x_{\mathrm{u}}/(k_{\mathrm{B}}T)), \tag{1}$$

where k_{u}^{0} denotes the unfolding rate at zero force, f denotes the force applied on the protein, x_{u} denotes the unfolding distance, k_{B} denotes the Boltzmann constant, and T denotes the absolute temperature. By using AFM, Brock *et al.* observed single step unfolding of PLY47W. They determined the unfolding distance to be $x_{\mathrm{u}} = 0.22$ nm and zero-force unfolding rate $k_{\mathrm{u}}^{0} = 0.06\ \mathrm{s}^{-1}$, at constant pulling speeds ranging from 40 nm/s to 4000 nm/s. In these experiments, average unfolding force ranged from 90 pN to 200 pN, while the observed unfolding events occurred at forces ranging from 50 pN to 250 pN.[10] By using MTs, Tapia-Rojoa *et al.* measured force-dependent unfolding rates of PLY47W at forces ranging from 15 pN to 35 pN,[13] determining the unfolding distance $x_{\mathrm{u}} = 0.44$ nm, and unfolding rate constant $k_{\mathrm{u}}^{0} = 0.0026\ \mathrm{s}^{-1}$. The different results obtained by AFM and MTs might be due to the large force range differences in AFM and MTs measurements. Therefore, a systematic measurement over a large force range is required to clarify this discrepancy. With the

†Corresponding author. E-mail: chenhu@xmu.edu.cn

© 2024 Chinese Physical Society and IOP Publishing Ltd

development of MTs,[15] the unfolding rate over a larger force range can be measured.

Furthermore, PLWT has not been studied by SMFS and the impact of Y47W mutant on the stability has not been explored. Recently, MTs have revealed multiple transition barriers along the unfolding pathway of various traditional two-state proteins, such as GB1, Csp, and AcP.[6,7,16] Protein L exhibits structural similarities to GB1[17] and their dynamics can be compared to each other in chemical and mechanical denaturation experiments to reveal some common properties.[18–20]

In this study, MTs were utilized to measure force-dependent folding and unfolding rates of both PLWT and PLY47W at forces ranging from 3 pN to 120 pN. The logarithmic force-dependent unfolding rate exhibits distinct slopes below 50 pN and above 60 pN, implying a general two-barrier unfolding pathway. The measurements showed an increase in the unfolding rate of PLY47W compared to PLWT, but both constructs exhibited similar folding rates. Free energy landscapes of both PLWT and PLY47W are constructed to show the effect of this mutation on the dynamics of protein L.

2. Materials and methods

2.1. Sample preparation

Flow chambers were created by sandwiching a piece of functionalized coverslip with another piece of coverslip, with a parafilm in-between to prevent leakage. Polybead amino microspheres (cat. 17145, Polysciences) with a diameter of 3.0 μm were introduced into the chamber to adhere to the coverslip. After rinsing with PBS buffer, 1% Sulfo-SMCC (SE 247420, Thermo Science) in PBS was introduced into the chamber and incubated for 20 min. Following that, SpyCatcher protein in PBS was introduced into the chamber to coat the functionalized surface for 1 hour.[21] Subsequently, 1% BSA in PBS at pH 7.4 was introduced into the chamber and incubated overnight at 4 °C to passivate the surface. Prior to the single molecule experiment, the chambers were incubated in PBS buffer with approximately 1 nM of protein L protein for 10 min. Finally, Streptavidin-coated paramagnetic beads Dynabead M270 (cat. 65305, Invitrogen) were introduced into the chamber to form protein tethers.

2.2. Magnetic tweezer measurement

At the beginning of each single molecule measurement, a library of images of the tethered bead and the reference bead at a series of focal planes every 50 nm were stored. During the measurement, the power spectrum of the bead images was compared with the image library to obtain changes in the tether extension with a resolution of less than 2 nm. To cancel drift, negative feedback was used to keep the focal plane of the reference bead at the same position. The forces applied on a paramagnetic bead (M270, Invitrogen) as a function of the distance d between the magnets and the sample chamber, $f(d)$, were calibrated using the method in previous work.[15]

The plasmid constructs, protein expression, and theoretical analysis are given in SI.

3. Results

3.1. Divergence in measurements with different loading rates

In the MT experiments, the protein construct was linked between a SpyCatcher-coated coverslip and a streptavidin-coated paramagnetic bead (Fig. 1(a)).[22] We initially applied a constant loading rate of 1 pN/s to pull the four tandem repeats of PLWT domain. During this process, four unfolding events characterized by sudden increases in extension were observed (Fig. 1(c)). When the force reached ∼ 75 pN, all four protein L domains unfolded. Subsequently, the loading rate was adjusted to −1 pN/s, allowing the protein L domains to refold back to their native states as the force dropped below 5 pN. Successful folding was confirmed by observing similar unfolding signals in the next stretching cycle. By performing multiple force-ramp cycles on different tethers, we obtained the unfolding force distribution of PLWT at loading rates of 1 pN/s and 0.2 pN/s, as shown in Fig. 1(d). The most probable unfolding forces were determined to be ∼ 63 pN at a rate of 1 pN/s and ∼ 48 pN at 0.2 pN/s.

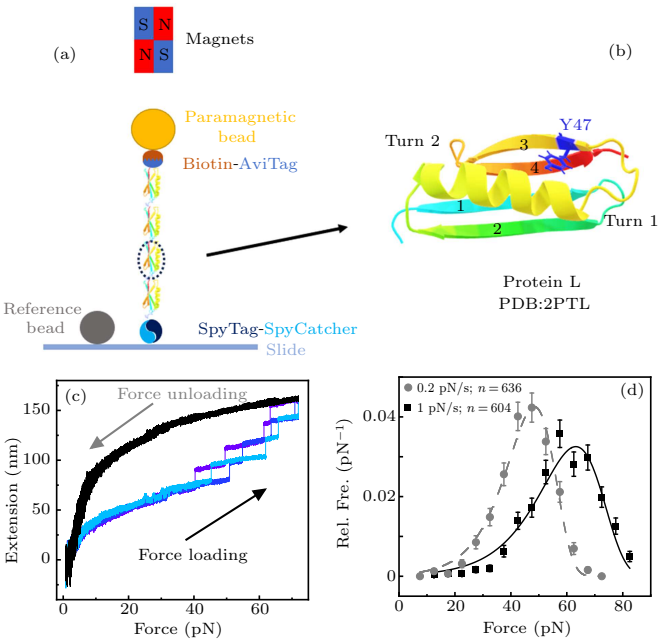


Fig. 1. Unfolding of PLWT in force-ramp experiments. (a) Sketch of MTs with a protein construct $PLWT_4$ linked between glass surface and a paramagnetic bead. (b) The three-dimensional structure of PLWT with residue Y47 highlighted in blue. (c) Force–extension curve of $PLWT_4$, measured in force-ramp experiments with constant loading and unloading rates of ±1 pN/s. Each extension jump step corresponds to an unfolding event of a PLWT domain. (d) The unfolding force distributions of PLWT at constant loading rate of 0.2 pN/s (black squares) and 1 pN/s (gray circles). The distribution is fitted by Eq. S1 with $k_u^0 = (8 \pm 2) \times 10^{-5}$ s^{-1} and $x_u = 0.47 \pm 0.02$ nm for 0.2 pN/s, and $k_u^0 = (3 \pm 1) \times 10^{-4}$ s^{-1} and $x_u = 0.36 \pm 0.02$ nm for 1 pN/s.

The force distributions were fitted with Eq. S1 and gave corresponding parameters: unfolding rate constant $k_u^0 = (8 \pm 2) \times 10^{-5}$ s^{-1} and unfolding distance $x_u = 0.47 \pm 0.02$ nm at loading rate of 0.2 pN/s, and $k_u^0 = (3 \pm 1) \times 10^{-4}$ s^{-1} and $x_u = 0.36 \pm 0.02$ nm at 1 pN/s. The divergence of fitting parameters at force loading rates of 0.2 pN/s and 1 pN/s indicates that Bell's model might not describe the unfolding dynamics of PLWT.[14]

3.2. Transitions over a large force range by force-jump measurement

To obtain force-dependent folding and unfolding rates over a large force range directly, we performed a force-jump experiment, as shown in Fig. 2(a). Initially, all four PLWT domains remained in their native state at 5 pN. Subsequently, the force was abruptly increased to 50 pN, each of four stepwise increases in extension ($\sim$ 18 nm) corresponds to an unfolding event. By applying a single exponential fitting to the unfolding probability as a function of time, unfolding rates were determined (Fig. S2). After all domains were unfolded at 50 pN, the force was decreased to 5 pN, followed by peptide contraction (due to its entropic elasticity) and protein folding process (peptide folds to native state). When the force was smaller than 5 pN, protein folding occurred with large extension fluctuations, making it difficult to identify each folding step. The folding rates at forces of 3 pN, 4 pN, and 5 pN were determined by fitting the average extensions with single exponential functions (Fig. 2(b)). These force-jump experiments were employed to measure the unfolding rates at forces ranging from 9 pN to 120 pN, and folding rates at force range of 3–5 pN.

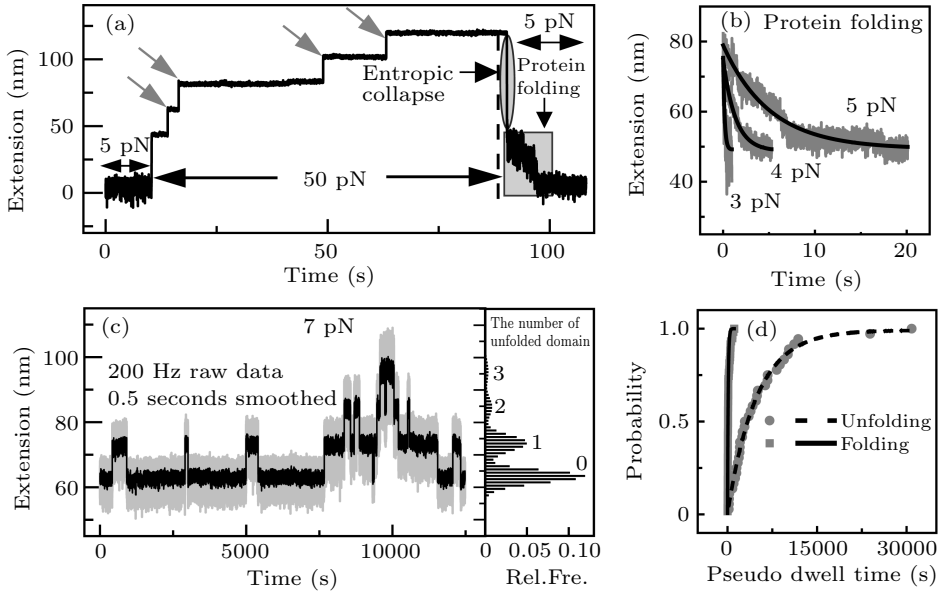


Fig. 2. Unfolding and refolding dynamics of PLWT$_4$ at constant forces. (a) The domains of PLWT$_4$ undergo stepwise unfolding when the force is increased from 5 pN to 50 pN, followed by entropic collapse of the peptide (gray circle area) and subsequent folding (gray square area) upon decreasing the force to 5 pN. (b) Exponential decay functions are used to fit the average folding time courses at 3 pN, 4 pN, and 5 pN obtained from more than four folding time courses, to obtain $k_f(f)$. (c) Equilibrium folding and unfolding dynamics of PLWT$_4$ are observed in the extension time course of 12000 s at 7 pN. Right panel shows the histogram of extension with distinct peaks corresponding to different numbers of unfolded domains. (d) The unfolding and folding probability of PLWT at 7 pN are obtained through cumulative distribution of pseudo-dwell time. The exponential fitting curves determine k_u and k_f of PLWT at 7 pN.

At force range of 6–8 pN, both folding and unfolding events PLWT can be recorded, as shown in Fig. 2(c). The time intervals between unfolding events or folding events are transformed into pseudo-unfolding or folding dwell times (Fig. S8).[6,23] The unfolding and folding probabilities as functions of time are derived from the cumulative distribution analysis of the pseudo-dwell times (Fig. 2(d)). The unfolding and folding rates at forces from 6 pN to 8 pN are then calculated by fitting the data to exponential functions. These rates are shown as open symbols in (Fig. 3(b)).

The histogram of extension reveals multiple peaks corresponding to varying numbers of unfolded protein L domains. The probability of having n unfolded domains in PLWT$_4$ construct, denoted as $P(n)$, can be directly read out from the extension distribution peaks (Fig. 2(c), right-hand panel), which should follow the binomial distribution: $P(n) = C_4^n p^n (1-p)^{4-n}$. Here $C_4^n = 4!/[n!(4-n)!]$ is the binomial coefficient, and the single free parameter p stands for the probability of a protein domain in an unfolded state. Fitting the binomial distribution to the normalized probability of the number of unfolded PLWT repeats gives $p = 0.14 \pm 0.05$ (Fig. S4). Therefore, $\Delta G(f = 7.0 \text{ pN}) = 1.8 \pm 0.1\ k_B T$ by (Eq. S2), which agrees well with the value obtained from the pseudo-dwell time analysis. The zero-force free energy difference, ΔG_0 is calculated to be $10.8 \pm 1.0\ k_B T$ using (Eq. S5).

3.3. Force-dependent transition rates and free energy landscape

The same measurements were done for both PLWT and PLY47W. The unfolding and folding rates of PLWT and PLY47W are summarized in Fig. 3(a). The data points are average values from at least three independent measurements.

First, the force-dependent folding rates exhibit striking similarity between PLWT and PLY47W. Similar to most proteins, folding rate is very sensitive to force, decreasing by four orders of magnitude within the force range of 3–8 pN, as illustrated in Fig. 3(b). The force-dependent folding rates follow Arrhenius' law Eq. S7 with $k_f^0 = 25\ s^{-1}$ and the size of folding transition state about 3.4 nm for both PLWT and PLY47W.

In contrast to the identical folding rate, PLY47W unfolds faster than PLWT, and the force-dependent unfolding rate of PLY47W exhibits an overall upward shift compared to that of PLWT. Additionally, the unfolding rates of both PLWT and PLY47W exhibit segmented linear relationship with force, and the slope below 50 pN is greater than that above 60 pN (Fig. 3(a)). For the force-dependent unfolding rates at forces greater than 60 pN, fitting with Bell's model gives the unfolding distances of $x_{u1} = 0.22 \pm 0.02$ nm for PLWT and 0.26 ± 0.03 nm for PLY47W (Figs. S5 and S7), which are almost the same within the fitting errors. When force is smaller than 50 pN, the same fitting gives $x_{u2} = 0.55 \pm 0.05$ nm for PLWT and 0.50 ± 0.05 nm for PLY47W, which is consistent with previous measurements by MTs.[13] Considering that PLWT and PLY47W share the same structures and similar unfolding distances at both high and low forces range (Fig. S5), we employed the globule fitting and shared the unfolding distances on their unfolding rates within force ranges of 6–50 pN and 60–120 pN, respectively, as shown in Fig. 3(a).

The extrapolated zero-force unfolding rates k_u^0 are highly dependent on the fitting parameter x_u, especially the fitting at high-force regime. To get more comparable fitting results of k_u^0 for PLWT and PLY47W, we fitted the force-dependent unfolding rates of PLWT and PLY47W with shared common parameter x_u, which gives $x_{u1} = 0.22$ nm and $x_{u2} = 0.54$ nm at high-force and low-force regimes, respectively (Fig. 3(a)). At high-force regime, the fitting gives $k_{u1}^0 = 4.8 \times 10^{-3}$ and $k_{u1}^0 = 1.5 \times 10^{-2}$ for PLWT and PLY47W, respectively. The same fitting at low-forces regime gives $k_{u2}^0 = 6.4 \times 10^{-5}$ and $k_{u2}^0 = 2.7 \times 10^{-4}$ for PLWT and PLY47W, respectively. Therefore, the overall unfolding rate of PLY47W is about 3–4 times faster than PLWT.

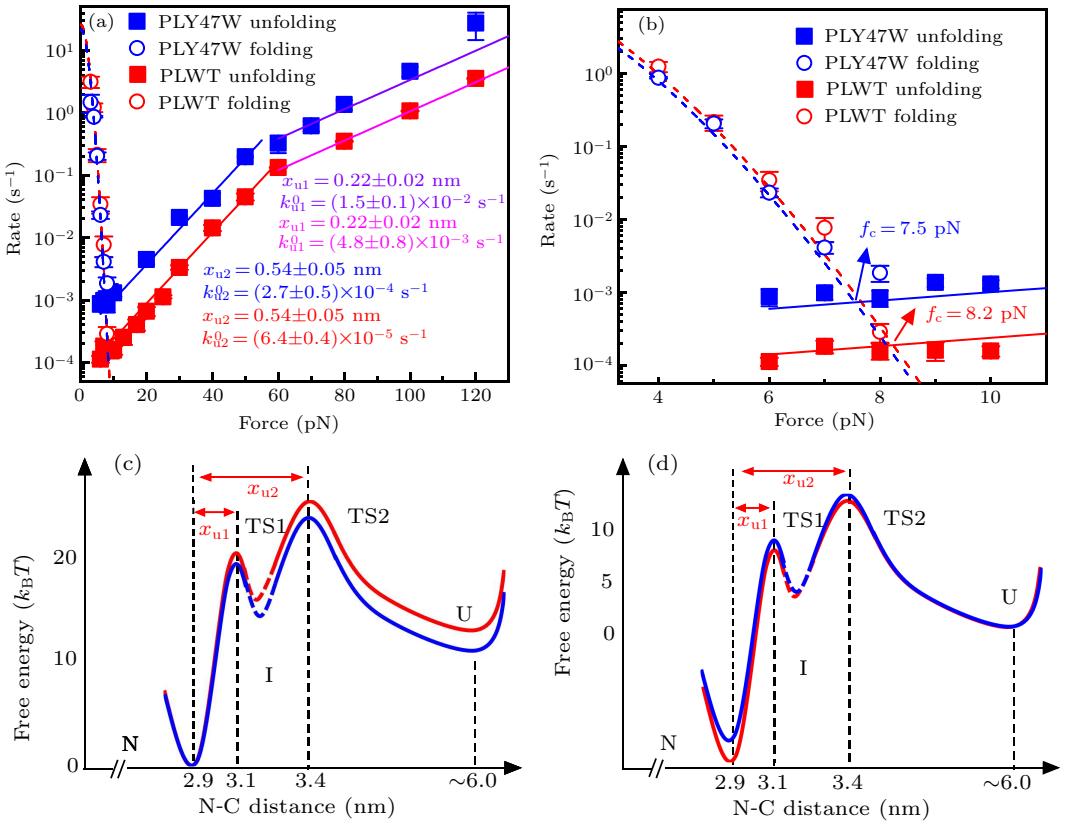


Fig. 3. Force-dependent folding/unfolding rates and free energy landscapes of PLWT and PLY47W. (a) Average unfolding (solid squares) and folding rates (empty circles) of PLWT (red) and PLY47W (blue) obtained from equilibrium and force-jump measurements of three independent protein tethers are shown at forces from 3 pN to 120 pN. Bell's model was used to fit the force-dependent unfolding rates with shared x_{u1} and x_{u2} at force ranges: 6–50 pN and 60–120 pN. (b) Enlarged figure at small forces shows the critical force of 8.2 pN and 7.5 pN for PLWT and PLY47W, respectively. The folding rates were analyzed using Arrhenius' law (Eq. S7). Error bars of rates indicate the standard error of the mean. (c) The free energy landscapes of PLWT (red) and PLY47W (blue) at zero force are plotted as a function of N–C distance, with the free energy of the native states as reference. (d) The free energy landscape with the unfolded state as reference.

The unfolding distance at forces below 50 pN is observably bigger than that at larger forces, which clearly reveals that there are two barriers along the unfolding pathway. The N–C distance refers to the distance between α carbon atoms of residues at N-terminus and C-terminus in a protein structure. Based on the N–C distances of the native states of PLWT (2.89 nm) and PLY47W (2.86 nm), and the unfolding distances of 0.22 nm at force range of 60–120 pN and of 0.54 nm at 6–50 pN. The size of unfolding transition state TS1 was estimated to be 3.1 nm. Similarly, the size of TS2 is about 3.4 nm, which is the same as the folding transition state. Therefore, at forces smaller than 8 pN, both folding and unfolding processes are crossing the same barrier TS2. The N–C distance of unfolded state is estimated from the root mean square (RMS) of the end-to-end distance vector of the polypeptide as a polymer: $\sqrt{\langle 2AL \rangle}$, where A denotes the persistence length (~ 0.8 nm) and L denotes the contour length (0.36 nm per amino acid and 63 amino acids).[24]

The crossing points of force-dependent folding and unfolding rates determine the critical forces, which are 8.2 pN and 7.5 pN for PLWT and PLY47W, respectively. From the critical forces and unfolding step size, the folding free energies of PLWT and PLY47W are calculated to be 11.7 $k_{\mathrm{B}}T$ and 10.2 $k_{\mathrm{B}}T$, respectively. Therefore, the mutant Y47W decreases the folding free energy by about 1.5 $k_{\mathrm{B}}T$.

If we set the intrinsic protein unfolding rate as $k^* = 10^6$ s^{-1} in the case of zero barrier, we can calculate the free-energy barriers ($\Delta G^{\dagger}$) of these transition states using an equation $k_{\mathrm{u}}^0 = k^* \exp\left(\Delta G^{\dagger}/(k_{\mathrm{B}}T)\right)$.[25] The unfolding free-energy barriers for TS1 and TS2 of PLWT are approximately 19.2 $k_{\mathrm{B}}T$ and 23.5 $k_{\mathrm{B}}T$, respectively. Similarly, the free-energy barriers of PLY47W are approximately 18.0 $k_{\mathrm{B}}T$ and 22.0 $k_{\mathrm{B}}T$ for TS1 and TS2, respectively (Fig. 3(c)). To elucidate the effect of the mutation Y47W on the folding dynamics of protein L, we set the free energy of the unfolded state as zero in Fig. 3(d). With the unfolded state as the reference, TS2 of PLY47W is almost identical to TS2 of PLWT.

4. Discussion

The force-bearing part of protein L is the hydrogen bonds between the first and fourth β-strands. The mutation point is on the third β-strand, which is not subject to stretching force directly before unfolding. It is surprising to discover that the Y47W mutant significantly accelerates the unfolding rate, increasing it by approximately three to four times. Mutation Y47W not only decreases the stability of native state but also weakens the interaction between the first and fourth β-strands.

Protein L shares the same topological structure with several model proteins for protein folding studies: GB1, NuG2, protein L, and Ubiquitin, though they have poorly conserved amino acid sequence. Previous studies have revealed that the force-dependent unfolding rates of GB1 exhibit a nonlinear behavior between 5–160 pN, with distinct force sensitivities below 10 pN and above 20 pN.[6] The unfolding distances of NuG2 have been revealed by optical tweezers and AFM at low and high force regimes, respectively, to be 0.61 nm and 0.25 nm.[26,27] Measurement for Ubiquitin has only been done by AFM at high force regime, which gives x_{u} of 0.14 nm[28] (Table 1). To summarize, all these proteins have longer x_{u} at low-force regime than high-force regime, which gives two barriers in the free energy landscape. Therefore, the topological structures play a crucial role in determining the overall properties of the free energy landscape and their folding and unfolding dynamics.

Table 1. Unfolding distances of proteins with similar structures.

Protein	x_{u} (high force)	x_{u} (low force)	Reference	Methods
PLWT	0.22 nm (60–120 pN)	0.55 nm (6–60 pN)	this article	MT
PLY47W	0.26 nm (50–120 pN)	0.50 nm (6–50 pN)	this article	MT
GB1	0.25 nm (15–140 pN)	1.0 nm (5–9 pN)	Ref. [6]	MT
NuG2	0.25 nm (60–140 pN)	0.61 nm (10–40 pN)	Refs. [26,27]	AFM OT
Ubiquitin	0.14 nm (50–100 pN)		Ref. [28]	AFM

5. Summary

Previous studies focus on the Y47W mutation of protein L due to its superior fluorescence property, but the folding and unfolding dynamics of PLWT has not been systemically studied. In summary, we measured force-dependent folding and unfolding rates of both PLWT and PLY47W by MTs over large force range of 3–120 pN. Our results show that PLY47W unfolds faster than WT, but has folding rate almost identical to PLWT. The force-dependent unfolding rates of both PLWT and PLY47W exhibit distinct force sensitivities below 50 pN and above 60 pN. Based on the experimental results, free energy landscapes with two barriers are constructed for both PLWT and PLY47W. Previous chemical denatured experiments conducted by David Baker *et al.* utilized stopped-flow to measure the folding and unfolding rates of PLY47W in denaturant solutions. Linear extrapolation on logarithmic coordinates yielded unfolding rate constant of 0.02 s^{-1} and folding rate constant of 60 s^{-1} in solution without denaturant. We extrapolated the force-dependent unfolding rate to zero-force, obtaining $k_{\mathrm{u1}}^0 = 0.015$ s^{-1} at 50–120 pN, with a zero-force folding rate of 25 s^{-1} for PLY47W. The chemical denaturation and single-molecule experiments conducted re-

vealed similar magnitudes of folding rate constant, and unfolding rate constant from measurement at high forces and high-concentration of denaturant for PLY47W. Given our ability to measure the unfolding rate under smaller forces, we obtained unfolding constant $k_{u2}^{0} = 2.7 \times 10^{-4}$ from our experimental results at a lower force range of 6–50 pN, which is significantly lower than that from the high-force or high-concentration denaturant data. Former SMFS of PLY47W obtained by AFM determined the unfolding distance $x_u = 0.22$ nm at force range of 90–200 pN,[10] which equals our results measured by MTs experiments at forces ranging from 60 pN to 120 pN. On the other hand, Tapia-Rojoa *et al*. utilized MTs to measure force-dependent unfolding rates of PLY47W within a different force range of 15–35 pN, and determined x_u of 0.44 nm,[13] which is close to our results (0.5 nm) measured by MTs experiments at forces ranging from 6 pN to 50 pN. All these experiment results reveal a two-barrier unfolding pathway model for both PLWT and PLY47W, and there should be a transient intermediate state between these two transition states, as shown in Figs. 3(c) and 3(d).

Acknowledgements

The authors thank Shimin Le from Xiamen University for valuable discussions. This work was supported by the National Natural Science Foundation of China (Grant Nos. 12174322 to HC and 12204124 to ZG), 111 Project (Grant No. B16029), the Graduate Scientific Research Foundation of Wenzhou University (Grant No. 3162023003034 to JH), and research grant from Wenzhou Institute.

References

[1] Moore P B, Hendrickson W A, Henderson R and Brunger A T 2022 *Science* **375** 507
[2] Bell G I 1978 *Science* **200** 618
[3] Perl D, Welker C, Schindler T, Schröder K, Marahiel M A, Jaenicke R and Schmid F X 1998 *Nat. Struct. Mol. Biol.* **5** 229
[4] Kim D E, Fisher C and Baker D 2000 *J. Mol. Biol.* **298** 971
[5] McCallister E L, Alm E and Baker D 2000 *Nat. Struct. Mol. Biol.* **7** 66973
[6] Guo Z, Hong H, Yuan G, Qian H, Li B, Cao Y, Wang W, Wu C and Chen H 2020 *Phys. Rev. Lett.* **125** 198101
[7] Hong H, Guo Z, Sun H, Yu P, Su H, Ma X and Chen H 2021 *Commun. Chem.* **4** 156
[8] Liu R, GarciaManyes S, Sarkar A, Badilla C L and Fernández J M 2009 *Biophys. J.* **96** 3810
[9] Plaxco K W, Simons K T and Baker D 1998 *J. Mol. Biol.* **277** 985
[10] Brockwell D J, Beddard G S, Paci E, West D K, Olmsted P D, Smith D A and Radford S E 2005 *Biophys. J.* **89** 506
[11] Sun H, Guo Z, Hong H, Yu P, Xue Z and Chen H 2021 *Biophys. Rep.* **7** 399
[12] Sun H, Guo Z, Hong H, Zhang Z, Zhang Y, Wang Y, Le S and Chen H 2023 *Phys. Rev. Lett.* **131** 218402
[13] TapiaRojo R, Eckels E C and Fernández J M 2019 *Proc. Natl. Acad. Sci. USA* **116** 7873
[14] Pierse C A and Dudko O K 2017 *Phys. Rev. Lett.* **118** 088101
[15] Chen H, Fu H, Zhu X, Cong P, Nakamura F and Yan J 2011 *Biophys. J.* **100** 517
[16] Ma X, Sun H, Hong H, Guo Z, Su H and Chen H 2022 *Phys. Rev. E* **106** 024404
[17] Wikstroem M, Drakenberg T, Forsen S, Sjoebring U and Bjoerck L 1994 *Biochemistry* **33** 14011
[18] O'Neill J W, Kim D E, Baker D and Zhang K Y 2001 *Acta Crystallogr. D* **57** 480
[19] Scalley M L, Yi Q, Gu H, McCormack A, Yates J R and Baker D 1997 *Biochemistry* **36** 3373
[20] Cao Y, Lam C, Wang M and Li H 2006 *Angew. Chem. Int. Ed.* **118** 658
[21] Guo Z, Hong H, Sun H, Zhang X, Wu C, Li B, Cao Y and Chen H 2021 *Nanoscale* **13** 11262
[22] Zakeri B, Fierer J O, Celik E, Chittock E C, SchwarzLinek U, Moy V T and Howarth M 2012 *Proc. Natl. Acad. Sci. USA* **109** E6907
[23] Chen H, Yuan G, Winardhi R S, Yao M, Popa I, Fernandez J M and Yan J 2015 *J. Am. Chem. Soc.* **137** 3540
[24] Marko J F and Siggia E D 1995 *Macromolecules* **28** 8759
[25] Best R B, Fowler S B, TocaHerrera J L and Clarke J 2002 *Proc. Natl. Acad. Sci. USA* **99** 12143
[26] Lei H, He C, Hu C, Li J, Hu X, Hu X and Li H 2017 *Angew. Chem. Int. Edit.* **56** 6117
[27] Cao Y, Kuske R and Li H 2008 *Biophys. J.* **95** 782
[28] Schlierf M, Li H and Fernandez J M 2004 *Proc. Natl. Acad. Sci. USA* **101** 7299